Multi-sensor data fusion for Additive Manufacturing process control

Ambra Vandone[1], Stefano Baraldo[1] and Anna Valente[1]

***Abstract*— Achieving cutting-edge mechanical properties of metal parts realized by Additive Manufacturing (AM) demands articulated process control strategies, due to the multitude of physical phenomena involved in this kind of manufacturing processes. Complexity is even higher for what concerns the Direct Energy Deposition (DED) technique, which offers much more potential flexibility and efficiency with respect to other metal AM technologies, at the cost of more difficult process control. The present work presents a multi-sensor approach able to combine on-line signals, collected while monitoring the deposition process, and data coming from off-line inspection devices, during the built part quality check phase. This data fusion approach constitutes the foundation for the process modelling phase and, consequently, for the implementation of an intelligent control strategy that would act on-line by adjusting the machine process parameters chasing part dimensional, mechanical and quality targets. The benefits of the proposed solution are assessed through a dedicated experimental campaign on a DED machine.**

I. INTRODUCTION

Additive Manufacturing (AM) brought terrific innovation in complex shape parts manufacturing. Unlike conventional techniques such as machining, which fabricates products by removing material from a larger stock, AM creates the final shape starting from a computerized 3D solid model and adding material, layer after layer. This allows to produce extremely customized parts, even with high geometrical complexity. Despite the multitude of appreciated benefits, improvements in process monitoring and control still have to be done for its stable adoption in industry. Among metal based AM technologies, the focus of this work is on *Direct Energy Deposition (DED)*, where a mixture of carrier gas and metal powder particles is blown out from a set of nozzles [1]. The particles intercept a laser beam that provides the necessary energy to fuse them and to form a *melt pool* [2], i.e. a drop of molten metal. While the deposition head advances, moving the nozzle and the laser beam according to the desired product geometry, the melt pool cools down, evolving into a solid metal *track*. A shielding gas prevents the metal oxidation and helps conveying the powder stream, enhancing the process efficiency. Fig. 1 illustrates schematically the process. If compared to other AM techniques, DED is one of the less investigated and mature, and the research and industrial worlds are currently lacking structured studies and analyses, process design/control methodologies and experimental data sets. This is mainly due to the high complexity of a process that involves several physical phenomena, ranging from fluid dynamics of the stream and heat dissipation to material growth and microstructure. Wide experience and process understanding are required to produce pieces complying their mechanical and geometrical requirements. Operators that are still facing the DED manufacturing challenge with a trial-and-error approach could be supported by a proper process control strategy, that, likely, would lead to minimizing waste, reducing faulty parts and post processing or repairing actions, and avoiding time-consuming testings.

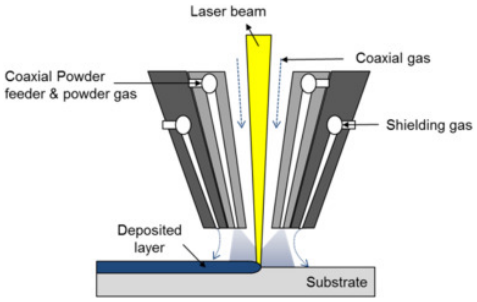

Fig. 1: Direct Energy Deposition process.

The present paper proposes a process control solution based on data-driven modelling. In particular, the process modelling phase relies upon the fusion of information extracted from data gathered off-line (3D shape of the deposited material) and on-line (melt pool images and machine tool trace). Successively, the control strategy acts on the machine control variables (laser power, tool velocity) to target the desired geometrical track dimensions (width, height), while optimizing the surface quality over time.

II. MOTIVATION

The majority of available DED machines are utilized by operators according to previously compiled look-up tables that suggest reasonable sets of process parameters for a coarse grid of target Key Performance Indicators (KPIs). Process modelling and control strategies could greatly help them to determine, in a shorter time, the optimal combinations of process parameters, and to maintain KPIs close to their desired values during the whole deposition. Given its complexity, multi-physics based models are still far from being practical or exhaustive in describing the DED process. As a consequence, researchers addressed their focus on models derived empirically by fitting data acquired either on-line, while monitoring the running deposition, or off-line, once the piece has been realized. Various authors [3] used linear models to correlate few process parameters and observable outcomes, though obtaining very different empirical models;

[1] SUPSI, University of Applied Science and Arts of Southern Switzerland, Department of Innovative Technologies; Via Cantonale 2, Manno CH-6928, Switzerland. ambra.vandone@supsi.ch; stefano.baraldo@supsi.ch; anna.valente@supsi.ch

this is a symptom that a simplistic approach is not sufficient to cover a wide variety of process conditions [4], [5].

Numerous solutions have been experimented for acquiring data during the deposition phase [6]. Optical devices are widely used, e.g. high-speed cameras that record frames of the melting area [7]. Vision monitoring systems are often integrated with temperature sensors such as thermal cameras or multi-wavelength pyrometers [8], [9]. However, these observable variables are only derived signals w.r.t. important, latent KPIs like deposited track width and inner porosity. This implies that a more comprehensive approach is required, establishing a correlation between what is observed on-line (monitoring data) and what are the real process outcomes (off-line inspection data).

In the present study, we propose an innovative data fusion approach that, for each time instant, associates on-line process and monitoring signals to the related latent process outcomes. This constitutes the key prerequisite to make the proposed control approach effective in adapting process parameters to the desired targets.

III. DATA FUSION APPROACH

The core of this work is represented by the fusion of different types of data, collected by a variety of devices, both during and after the deposition process. Examples of data that can be exploited, depending on available equipment, are:

- **On-line monitoring**: image features and statistics (e.g. melt pool diameter, average image brightness) from visible light cameras; thermal measurements.
- **On-line machine tracing**: current laser power, current laser spot position and speed from machine PLC.
- **Off-line inspection**: 3D surface reconstruction from stereoscopic systems, volume reconstruction from computed tomography, porosity from microscopy on cut samples.

These data can be either time- or space-referenced, in both cases at various different resolutions. Due to their heterogeneity, a comprehensive data fusion approach is necessary to fully exploit this wealth of information. In particular, Fig. 2 illustrates the approach we developed taking into account the data available through our experimental setup: as detailed in Sections III-B and III-C, during experimental runs, laser power and spot coordinates are logged by the machine PLC, while a camera acquires melt pool images at high speed; moreover, after each deposition run, a 3D scan of the resulting sample geometry is performed; these data are then registered in time and space, thus composing an integrated data set. This work flow could be easily extended to manage similarly other types of information.

The final outcome of the data fusion procedure is the estimated process model, which encloses the process knowledge collected during the preliminary experimental campaign. The model is then used during on-line process control, as described in Section III-E.

A. Experimental setup

The experimental infrastructure exploited for the present work is composed by a Prima Power Laserdyne 430 3-axis CNC machine, originally designed for laser cutting operations, and converted by the research group to an AM machine through the integration of a four-nozzle Optomec DED head, and equipped with a FLIR high speed camera. The camera is mounted onto the deposition head and, thanks to the insertion of a dichroic mirror in the optical chain, it allows for on-line monitoring of the melt pool area. Off-line measurements are performed using a GOM ATOS Core 200 fringe projection scanner, that provides a 3D mesh representing the built part surface. All the equipment components are shown in Fig. 3.

To guarantee the usefulness of a data fusion approach for industrial machines, the required preliminary experimental campaign should be straightforward to execute, and automatic elaboration routines should exist. In this spirit, we focus on a data assimilation methodology based on simple experiments like single tracks of material deposited with different machine settings, which are analyzed automatically by a chain of computer vision techniques - described in detail in the next two Sections - that provides the KPIs used in this work:

- **height and width of deposited single tracks**, to be compared with application-specific target values;
- **track surface roughness** (see Section III-D), which must be minimized by the control model;
- **average image intensity and number of sparks**, which are extracted from the melt pool video stream and can be considered as proxy observations of track quality.

B. Vision processing

During each single track depositions, images representing the melt pool area and cropped at a resolution of 384x384 pixels have been captured by means of the FLIR camera. This frame dimension allows to visualize all the features we consider of relevance, i.e. the area heated by the laser beam and the sparks departing from it, but also to appreciate the process dynamics by enabling an acquisition rate up to 120 Hz. Frames transferred to a PC have been elaborated by a dedicated image processing algorithm developed to face two main issues: image correction and feature extraction.

First of all, a correction of image intensity resulted necessary to compensate the increase of brightness caused by the fusion vapours under certain test conditions. These vapours entrap the radiation coming from the substrate, creating a bright halo that could impair the feature extraction process. For each captured frame, pixel intensity distribution has been analyzed and, among various statistical parameters, the asymmetry - evaluated through the skewness factor [10] - has been kept into consideration: since a negative skewness value identifies images mainly composed by brighter pixels, it reveals the misleading increased light intensity. To compensate this artifact, a corrective factor has been defined, proportional to the the difference of background intensity between images captured while the laser beam was turned on and off. After the brightness correction, the average light intensity for the

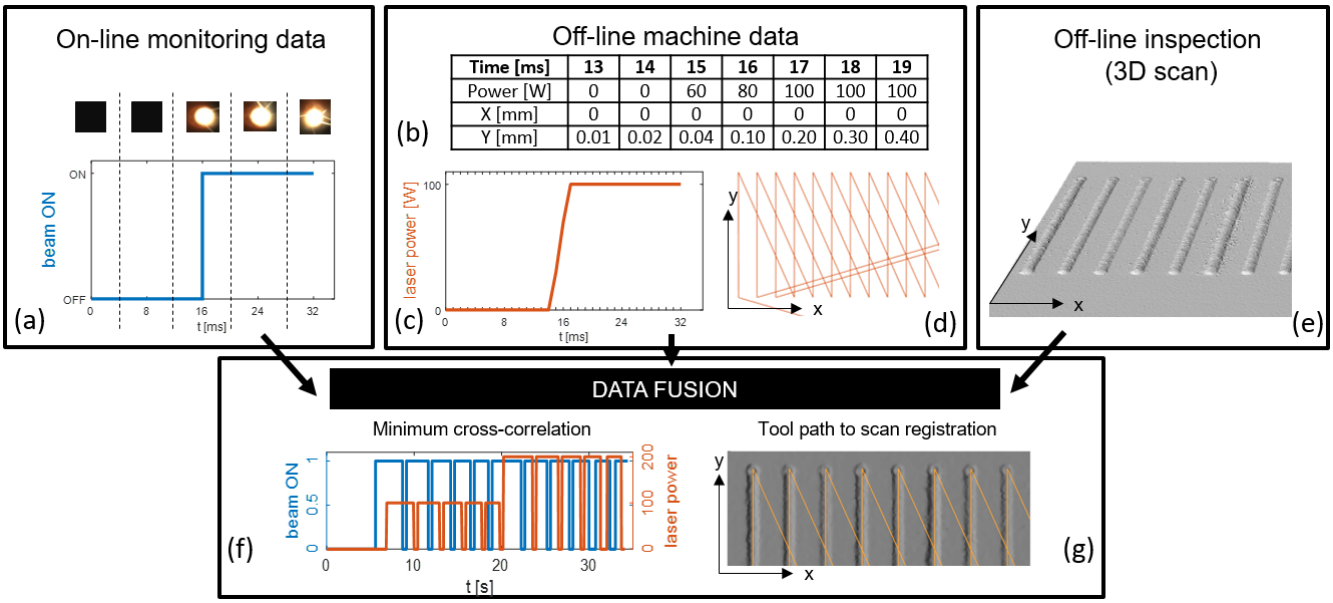

Fig. 2: Data fusion approach: in the machine log file (b) laser power and tool position are recorded at each time stamp. This information allows for the time-alignment (f) of the melt pool images through the computation of the cross-correlation between the laser power signal (c) and the image retrieved beam-ON signal (a), and the spacial registration (g) of the 3D deposited geometry (e) to the tool trace (d).

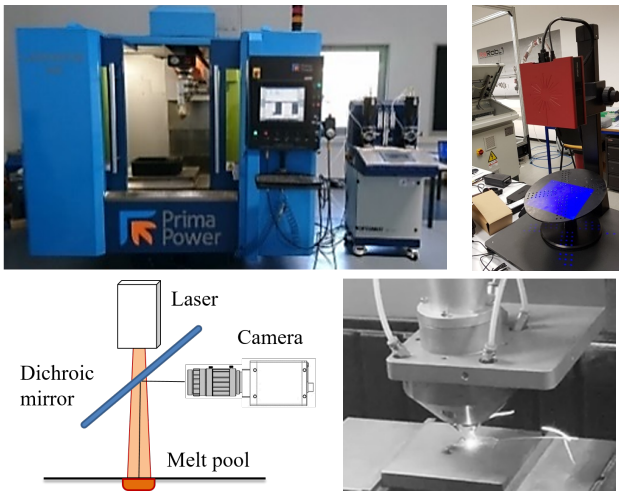

Fig. 3: Equipment setup: DED machine (top left), 3D scanner (top right), high speed camera setup (bottom left) and deposition head (bottom right).

whole frame has been stored as an indicator of the overall emitted radiation.

Secondly, image analysis has been carried out to detect relevant features. A two-level intensity threshold algorithm has been developed to extract the melt pool area and surrounding heated zone out of the background. Primary importance has been addressed to the tuning of the threshold level: hundreds of images randomly picked from the deposition tests have been selected to constitute a training data set for an algorithm based on Otsu's method [11]. Then, pixels having an intensity value higher than the first estimated threshold level have been considered representative of the heated zone, while pixels exceeding even the second level have been considered representative of the melted area, whose extension have been computed. To extract information related to sparks, instead, an adaptive local threshold approach has been developed, since sparks are constituted by pixels extremely varying in intensity levels and potentially located anywhere in the image. The intensity gradient computed on a 21x21 pixel kernel and superimposed consequently to each pixel enabled to emphasize and detect bright spots. Morphological filters [12] applied to these spots helped separating different spots; moreover, only those presenting critical shape extension and elongation have been flagged as sparks. The number of sparks for each image has been computed and saved. Fig. 4 presents the results of the image processing applied in two different laser power conditions: 600 W for the left image, and 900 W for the right image.

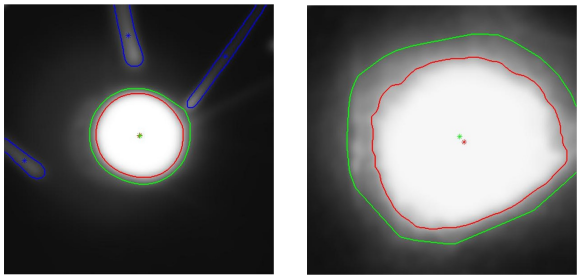

Fig. 4: Melt pool image processing: melt pool area and centroid (red marks), heated area and centroid (green marks), detected sparks (blue marks).

Finally, the registration of vision signals to the deposition

tool path has been performed aligning the laser power signal recorded in the machine log file to a *laser ON* signal deduced from melt pool presence in video frames, by minimizing the cross-correlation between the two signals.

C. 3D scan processing and signal alignment

The surface mesh representing the deposited material constitutes the ground truth for the geometry KPIs. The proposed data fusion approach requires the integration of time- and space-referenced data: to this aim, on the mesh we segment the deposited material from the substrate, so that the alignment of this sub-mesh to the machine tool path can be used to provide a time stamp to geometric features identified on the scan. Since DED samples present irregular substrates due to isolated fused powder grains, usual methods for plane identification have been improved to ignore these random spikes.The registration of the tool path to the corresponding deposited material has been achieved through a preliminary rough registration, based on main inertial axes, followed by a fine one. Given the peculiarity of this alignment task, i.e. fitting a "skeleton" trajectory inside a larger cloud of points (the sub-mesh vertices), we developed a new fine registration method, which evolves the approach of ICP [13] algorithms to align the trajectory in a barycentric position with respect to the deposited material. A detail of the result is presented in panel (g) of Fig. 2.

Once the trajectory is registered to the deposited tracks, the 3D mesh can be cut at arbitrary positions through planes perpendicular to the substrate and to the tool path velocity vector, thus generating 2D profiles that are both space- and time-referenced. These profiles can be processed to extract relevant geometric KPIs: in our specific setup, where single tracks have been used as reference deposition geometries, they are transverse track height and width. This has been achieved by developing a track identification algorithm that looks for large bell-shaped geometries in the mesh cut profiles, again ignoring irregularities induced by random grains (Fig. 5).

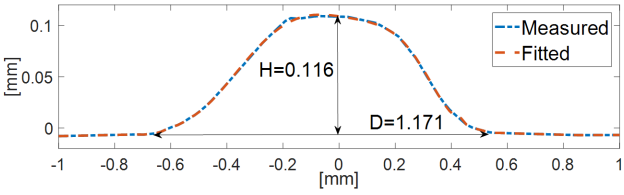

Fig. 5: Profile analysis: track width, height and roughness estimation.

Thanks to the proposed approach, the geometric features extracted from "static" data become time-referenced, in the perspective of correlating process parameters and monitoring data to the final deposition results. To this aim, eventually three pieces of information are merged: 3D mesh, melt pool images and machine motion parameters. The "bridging" function of the tool trace allows to associate process parameters, vision-extracted features and spacial 3D features by aligning them all to the trace itself. This level of integration of heterogeneous information represents the most comprehensive data fusion approach conceived for AM machines.

D. Data-driven modelling

To apply an effective integration of process knowledge into machine intelligence, it is necessary to estimate two sub-models: an *open-loop* component, i.e. the relation between process parameters and track features, and a closed-loop one, which represents the relation between on-line monitoring signals and unmodelled track quality features.

The open-loop process model determines the most suitable process parameters, i.e. laser power P and tool velocity V, necessary to realize a geometry that matches the target one. Track size has a huge importance in AM, since it characterizes the resolution of geometric features [14]. For example, a persistent 10% error in the height of single tracks induces a 10% error for the overall part height, implying either the need for additional corrective depositions, or higher waste due to corrective ablation, or even failure of the final part. Track width has a similar impact and induces even more unpredictable geometric aberrations. For this reason, maintaining cross-sectional dimensions as close as possible to the target values is essential in AM processes.

The width D and the height H of the track can be expressed as functions of the DED machine parameters:

$$\begin{aligned} d &= a_0 + a_p p + a_v v \\ h &= b_0 + b_p p + b_v v \end{aligned} \tag{1}$$

or, in matrix formulation, $x = Au + b$, where $x = (d,h)^T$ and $u = (p,v)^T$. Variables d, h, p and v are indicated in lower case, to represent the logarithm of the corresponding variable stated in capital. The formulation is open for integration of other parameters in the process model (e.g. spot size, powder flow rate), although the sake of simplicity we only focus on power and velocity.

On the other side, the closed-loop component should take into account KPIs that cannot be controlled by an open-loop approach, but that can be monitored indirectly by relying on real-time sensor data. Examples are surface roughness and yield strength, which are known to depend not only on process parameters but also on the specific tool path and thermal history of the manufactured part. To integrate such closed-loop control element, we propose the estimation of a *track degradation index* G as a function of the vector of real-time observed variables $\mathbf{y}$. In the present work, we consider $y = (i,n)^T$, where i represents the average intensity of a melt pool image and n represents the number of detected sparks, while the chosen track degradation index G is the standard deviation of the residuals between the measured profiles and their smooth fitting with a 4th degree polynomial (see Fig. 5). The relation between G and $\mathbf{y}$ can be established for example by estimating a linear model (see Section IV-A):

$$G(\mathbf{y}) = C\mathbf{y} + e. \tag{2}$$

E. Knowledge-based process control

The control strategy allows to identify the best process parameters to obtain a built part in compliance with the target

geometry and the required surface quality. The adoption of an on-line, knowledge-based process control represents a huge step forward in the management of manufacturing machinery, as commercial machines work with an open-loop approach, using parameters chosen by the operator after cumbersome tuning campaigns. The proposed approach consists in minimizing on-line, at each time step k, the following functional:

$$F(\mathbf{u}_k) = ||\bar{\mathbf{x}}_k - (A\mathbf{u}_k + b)||^2 + \lambda G(\mathbf{y}_{k-1})||Q\mathbf{u}_k||^2 + ||W(\mathbf{u}_k - \mathbf{u}_{k-1})||^2, \quad (3)$$

where Q is a projection matrix that selects the process parameter combination correlated with G. The functional (3) is composed by:

1) a least-squares term, based on the data-driven process model (1); this term forces the process to track the target KPIs (track log-width d and log-height h, in this application), which are not observable during the deposition process;
2) a penalty term for high values of the track degradation index G (a roughness measure described in Section III-D), which drives accordingly the variation of process parameters towards the direction indicated by the projection matrix Q; this term, characterized by the empirical model (2), allows to optimize track quality based on the on-line monitorable KPIs;
3) a term that penalizes high rates of variation of process parameters, to tune a smooth adaptation of u_k thanks to the (diagonal) weight matrix W.

A diagram of the closed-loop control approach arising from the described optimization strategy is presented in Figure 6.

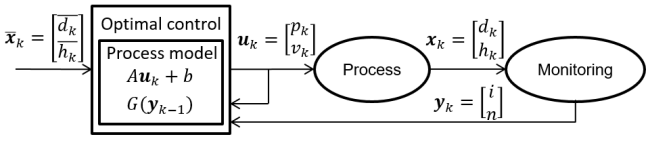

Fig. 6: Control loop diagram.

IV. MODEL VALIDATION AND EXPERIMENTAL RESULTS

A. Process model validation

The validation of the proposed approach relies upon the experimental campaign conducted with stainless steel (AISI 316L) powders with grain size in the range of 80 to 120 μm. 50 single tracks of 20 mm length have been deposited on the same substrate, using 10 equally spaced laser power levels between 100 W and 1000 W. Five equally spaced scanning feed rates, i.e. the velocity at which the deposition head translates the laser spot over the substrate, are associated to each laser power level from 400 mm/min up to 800 mm/min. For such analysis, the flow rate of the powder-carrier mixture (0.031 g/s) and the laser spot size (1 mm) have been kept constant. The process model has been determined by exploiting two linear regressions that relate the logarithms of profile geometry variables d and h to the logarithms of process parameters p and v. Such approach results quite representative of the actual process, yielding R^2 indices greater than 0.9 and detecting both the process parameters as significant. The performance of the regression model has been also assessed against more flexible fitting models. In particular, a Neural Network approach consisting of ten neurons and one hidden layer provides a good matching between data and model prediction. The linear regression and the NN show comparable performances (Fig. 7), supporting the choice of the simpler but equally effective linear regression approach.

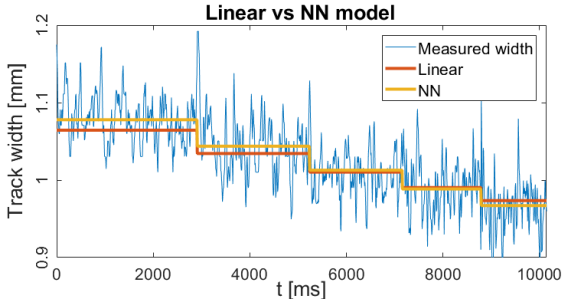

Fig. 7: Detail of comparison between linear and NN process models: measured track width (blue line), linear fitting (red line), and NN fitting (orange line).

Moreover, the track degradation index G has been found to be correlated both with a combination of the vision KPIs (the linear model $G(\mathbf{y}) = C\mathbf{y} + e$ has an R^2 index equal to 0.68 and both average intensity i and number of sparks n are significant variables with p-value <2e-6) and with the power density P/V (Pearson correlation coefficient $\rho = 0.9241$). To drive the control in the direction of power density, the projection matrix Q presented in (3) has been chosen as:

$$Q = \begin{bmatrix} 1/\sqrt{2} & -1/\sqrt{2} \\ 0 & 0 \end{bmatrix},$$

so that $Q\mathbf{u} = (p - v, 0)^T/\sqrt{2} = (log(P/V), 0)^T/\sqrt{2}$.

B. Control approach testing

Due to technological bottlenecks, the control strategy has been so far tested through simulations in the following conditions:

- track dimensions have been sampled by the estimated regression model, adding a Gaussian noise comparable to the one observed in the experiments;
- to simulate the variation of roughness during the process and its effect in terms of image intensity and generated sparks, two regression models have been estimated, to generate the roughness G from (p, v) and the image features (i, n) from G.

The proposed control approach has been applied to the simulated signal, imposing different target dimensions and initial power and velocity conditions. The results of one of these tests are displayed in Fig. 8. In this example, target

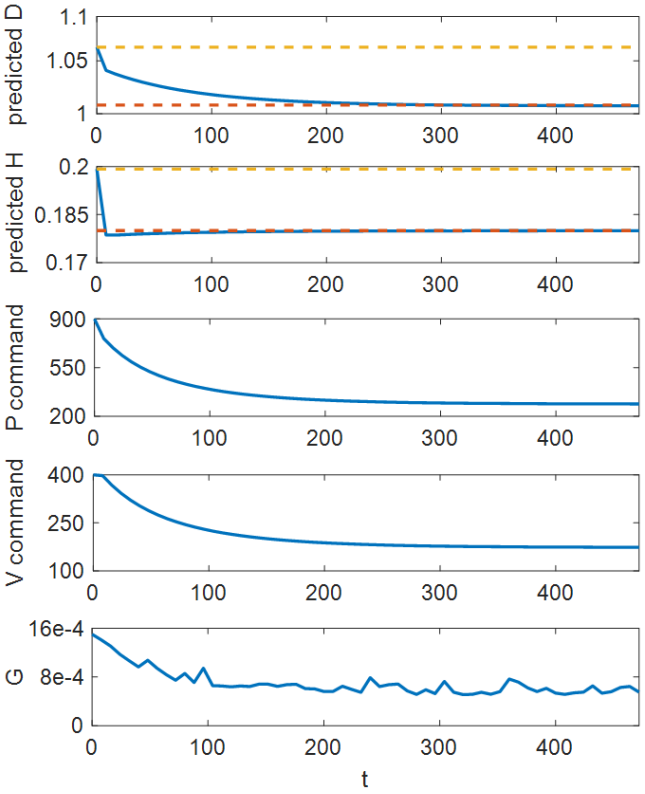

Fig. 8: Simulation results.

values $D = 1$ mm and $H = 0.18$ mm have been set, along with initial process parameter values $P_0 = 900$ W and $V_0 = 600$ mm/min, which yield initial sizes $D_0 = 1.0652$ mm and $H_0 = 0.1992$ mm. The first two panels in Fig. 8 show that, according to the prediction model, the correct dimensional features (orange dashed lines) are reached very fast (1% error reached in about 50 ms), while the remaining transient, about 300 ms, is a quality optimization phase, where the power density is adapted basing on the quality index G, which in turn converges to a value corresponding to about 1/3rd of the initial one. The convergence speed can be tuned coherently with the performances of the equipment, i.e. maximum scan acceleration and maximum power variation rate. A traditional open-loop approach based on the experience of a human operator, with inexact initial process parameter values, would maintain the initial, biased dimensional KPIs (yellow dashed lines) and would not reduce the initial roughness G, thus leading to a part not matching the quality requirements.

V. CONCLUSION

This paper proposes a novel approach for integrating heterogeneous AM process data, with the aim of evolving AM machines to autonomous, intelligent systems. The benefits of the approach have been assessed with regards to a specific machine setup: by printing a deposition plate of 50 tracks (about 2 minutes 40 seconds of lead time) it is possible to generate process models that provide effective prediction and control, despite their low (but increasable) level of complexity. This is a promising result towards an efficient scalability to different machine setups. Under the chosen test conditions, the proposed control model enables the adaptation of machine parameters in 50 ms, thus allowing to target a number of part quality KPIs (e.g. superficial roughness and 3D geometry). Future works will focus on:

- integration of powder stream dynamics (powder-carrier flow rate) and microstructural KPIs like porosity, which could be integrated with the very same registration approach presented in Section III-C;
- validation of the process on Laserdyne machine by running the control model in the machine CNC;
- integration of more geometric features by experiments of increasing complexity, from circular- and angular-shaped single tracks to net shape workpieces.

ACKNOWLEDGMENT

The research in this paper has been partially funded by EU H2020-FoF-2015, SYMBIONICA Next Generation Bionics And Smart Prosthetics. Contract 678144.

REFERENCES

[1] S. M. Thompson, L. Bian, N. Shamsaei, and A. Yadollahi, "An overview of Direct Laser Deposition for additive manufacturing; Part I: Transport phenomena, modeling and diagnostics," *Additive Manufacturing*, vol. 8, pp. 36–62, 2015.

[2] M. Schmidt, M. Merklein, D. Bourell, D. Dimitrov, T. Hausotte, K. Wegener, L. Overmeyer, F. Vollertsen, and G. N. Levy, "Laser based additive manufacturing in industry and academia," *CIRP Annals - Manufacturing Technology*, vol. 66, no. 2, pp. 561–583, 2017.

[3] A. J. Pinkerton, "Advances in the modeling of laser direct metal deposition," *Journal of Laser Applications*, vol. 27, no. S15001, 2015.

[4] A. Fathi and A. Mozaffari, "Vector optimization of laser solid freeform fabrication system using a hierarchical mutable smart bee-fuzzy inference system and hybrid NSGA-II/self-organizing map," *Journal of Intelligent Manufacturing*, vol. 25, no. 4, pp. 775–795, aug 2014.

[5] M. Akbari, S. Saedodin, A. Panjehpour, M. Hassani, M. Afrand, and M. J. Torkamany, "Numerical simulation and designing artificial neural network for estimating melt pool geometry and temperature distribution in laser welding of Ti6Al4V alloy," *Optik*, vol. 127, no. 23, pp. 11 161–11 172, 2016.

[6] T. Purtonen, A. Kalliosaari, and A. Salminen, "Monitoring and adaptive control of laser processes," *Physics Procedia*, vol. 56, pp. 1218–1231, 2014.

[7] S. Ocylok, E. Alexeev, S. Mann, A. Weisheit, K. Wissenbach, and I. Kelbassa, "Correlations of melt pool geometry and process parameters during laser metal deposition by coaxial process monitoring," *Physics Procedia*, vol. 56, pp. 228–238, 2014.

[8] L. Song, V. Bagavath-Singh, B. Dutta, and J. Mazumder, "Control of melt pool temperature and deposition height during direct metal deposition process," *International Journal of Advanced Manufacturing Technology*, vol. 58, no. 1-4, pp. 247–256, 2012.

[9] A. Vandone, P. Rizzo, and M. Vanali, "Two-stage automated defect recognition algorithm for the analysis of infrared images," *Research in Nondestructive Evaluation*, vol. 23, no. 2, pp. 69–88, 2012.

[10] W. H. Press, S. a. Teukolsky, W. T. Vetterling, and B. P. Flannery, *Numerical Recipes 3rd Edition: The Art of Scientific Computing*. Cambridge University Press, 2007, vol. 1.

[11] N. Otsu, "A Threshold Selection Method from Gray-Level Histograms," *IEEE Transactions on Systems, Man, and Cybernetics*, vol. 9, no. 1, pp. 62–66, 1979.

[12] R. C. Gonzalez, R. E. Woods, and S. L. Eddins, *Digital Image Processing Using Matlab*. Pearson Education, 2004.

[13] P. Besl and N. McKay, "A Method for Registration of 3-D Shapes," *IEEE Transactions on Pattern Analysis and Machine Intelligence*, vol. 14, no. 2, pp. 239–256, 1992.

[14] H. Qi, M. Azer, and P. Singh, "Adaptive toolpath deposition method for laser net shape manufacturing and repair of turbine compressor airfoils," *International Journal of Advanced Manufacturing Technology*, vol. 48, no. 1-4, pp. 121–131, 2010.